Newly synthesized anticancer drug HUHS1015 is effective on malignant pleural mesothelioma

Yoshiko Kaku,[1] Hisao Nagaya,[2] Ayako Tsuchiya,[1] Takeshi Kanno,[1] Akinobu Gotoh,[2] Akito Tanaka,[3] Tadashi Shimizu,[3] Syuhei Nakao,[3] Chiharu Tabata,[4] Takashi Nakano[4] and Tomoyuki Nishizaki[1]

[1]Division of Bioinformation, Department of Physiology, Hyogo College of Medicine, Nishinomiya; [2]Laboratory of Cell and Gene Therapy, Institute for Advanced Medical Sciences, Hyogo College of Medicine, Nishinomiya; [3]Laboratory of Chemical Biology, Advanced Medicinal Research Center, Hyogo University of Health Sciences, Kobe; [4]Department of Thoracic Oncology, Hyogo College of Medicine, Nishinomiya, Japan

The newly synthesized naftopidil analogue HUHS1015 reduced cell viability in malignant pleural mesothelioma cell lines MSTO-211H, NCI-H28, NCI-H2052, and NCI-H2452, with the potential greater than that for the anticancer drugs paclitaxel or cisplatin at concentrations higher than 30 μM. HUHS1015 induced both necrosis and apoptosis of MSTO-211H and NCI-H2052 cells. HUHS1015 upregulated expression of mRNAs for Puma, Hrk, and Noxa in MSTO-211H and NCI-H2052 cells, suggesting HUHS1015-induced mitochondrial apoptosis. HUHS1015 clearly suppressed tumor growth in mice inoculated with NCI-H2052 cells. Taken together, the results of the present study indicate that HUHS1015 could be developed as an effective anticancer drug for treatment of malignant pleural mesothelioma.

Malignant pleural mesothelioma is an aggressive and lethal tumor arising from previous asbestos exposure, yet disappointingly, little effective therapy has been provided. Naftopidil, an α_1-adrenoceptor blocker, has been clinically used for treatment of benign prostate hyperplasia and hypertension. We have found that naftopidil induces apoptosis in malignant mesothelioma cells by activating caspase-8 and the effector caspase-3, regardless of α_1-adrenoceptor blocking.[1] To obtain a more effective anticancer drug, we have newly synthesized the naftopidil analogue HUHS1015 (Fig. 1). HUHS1015 induced apoptosis of not only human malignant mesothelioma cell lines MSTO-211H, NCI-H28, NCI-H2052, and NCI-H2452 cells but also lung cancer cell lines A549, SBC-3, and Lu-65 cells, hepatoma cell lines HepG2 and HuH-7 cells, gastric cancer cell lines MKN-28 and MKN-45 cells, and bladder cancer cell lines 253J, 5637, KK-47, TCCSUP, T24, and UM-UC-3 cells, prostate cancer cell lines DU145, LNCap, and PC-3 cells, and renal cancer cell lines ACHN, RCC4-VHL, and 786-O cells.[2]

The present study aimed to assess whether HUHS1015 could be developed as a promising drug for treatment of malignant pleural mesothelioma. We show here that HUHS1015 exhibits a beneficial anticancer effect on malignant pleural mesothelioma.

Materials and Methods

Animal care. All procedures were approved by the Animal Care and Use Committee at Hyogo College of Medicine (Nishinomiya, Japan) and were in compliance with the National Institutes of Health Guide for the Care and Use of Laboratory Animals.

Cell culture. Human malignant pleural mesothelioma cell lines MSTO-211H, NCI-H28, NCI-H2052, and NCI-H2452 were purchased from ATCC (Manassas, VA, USA). Cells were grown in RPMI-1640 medium supplemented with 0.003% (w/v) L-glutamine, 10% (v/v) heat-inactivated FBS, penicillin (final concentration, 100 U/mL), and streptomycin (final concentration, 0.1 mg/mL), and incubated in a humidified atmosphere of 5% CO_2 and 95% air at 37°C.

Cell viability. Cell viability was evaluated by the MTT method as previously described.[1]

Cell cycle analysis. Before and after 24-h treatment with HUHS1015 (10 μM) or paclitaxel (10 μM), MSTO-211H, and NCI-H2052 cells were harvested by a trypsinization and fixed with 70% (v/v) ethanol at 4°C overnight. Fixed cells were incubated in PBS containing 1.5 μg/mL RNase A for 1 h at 37°C, followed by staining with 50 μg/mL of propidium iodide (PI) for 20 min on ice. Then, cells were collected on a nylon mesh filter (pore size, 40 μm), and cell cycles were
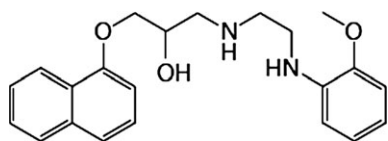

Fig. 1. Chemical structure of HUHS1015.

Table 1. Primers used for real-time RT-PCR

Bad	Sense	GCACAGCAACGCAGATGC
	Antisense	AAGTTCCGATCCCACCAGG
Bax	Sense	CGGACCCGGCGAGAGGC
	Antisense	TCAGCTTCTTGGTGGACGCATCC
Bid	Sense	CTACGATGAGCTGCAGACTG
	Antisense	GATGCTACGGTCCATGCTGTC
PUMA	Sense	GACGACCTCAACGCACAGTA
	Antisense	AGGAGTCCCATGATGAGATTGT
Hrk	Sense	TGCTCGGCAGGCGGAACTTGTAG
	Antisense	CTTTCTCCAAGGACACAGGG
Noxa	Sense	GCAGAGCTGGAAGTCGAGTG
	Antisense	GAGCAGAAGAGTTTGGATATCAG
Bcl-2	Sense	TCCGCATCAGGAAGGCTAGA
	Antisense	AGGACCAAGGCCTCCAAGCT
Bcl-X_L	Sense	TGGAATTCATGTCTCAGAGCAACCGGGAGC
	Antisense	CAGAATTCTCATTTCCGACTGAAGAGTGAGC
Mcl-1	Sense	GGACATCAAAAACGAAGACG
	Antisense	GCAGCTTTCTTGGTTTATGG
GAPDH	Sense	GACTTCAACAGCGACACCCACTCC
	Antisense	AGGTCCACCACCCTGTTGCTGTAG

assayed with a flow cytometer (FACSCalibur; Becton Dickinson, Franklin Lakes, NJ, USA) at an excitation of 488 nm and an emission of 585 nm, and analyzed using BD CellQuest Pro software (Becton Dickinson).

Apoptosis assay. Before and after 24-h treatment with HUHS1015 (15 μM) or paclitaxel (15 μM), MSTO-211H and NCI-H2052 cells were suspended in a binding buffer and stained with both PI and annexin V–FITC, and loaded on a flow cytometer (FACSCalibur) available for FL1 (annexin V)

and FL2 (PI) bivariate analysis. Data from 20 000 cells/sample were collected, and the quadrants were set according to the population of viable, unstained cells in untreated samples. CellQuest analysis of the data was used to calculate the percentage of the cells in the respective quadrants.

Real-time RT-PCR. Before and after treatment with HUHS1015 (15 μM) or paclitaxel (15 μM), total RNAs from MSTO-211H and NCI-H2052 cells were purified by an acid/guanidine/thiocyanate/chloroform extraction method using the Sepasol-RNA I Super kit (Nacalai, Kyoto, Japan). After purification, total RNAs were treated with RNase-free DNase I (2 units) at 37°C for 30 min to remove genomic DNAs, and 10 μg RNAs was resuspended in water. Then random primers, dNTP, 10× RT buffer, and Multiscribe Reverse Transcriptase were added to an RNA solution and incubated at 25°C for 10 min followed by 37°C for 120 min to synthesize the first-strand cDNA. Real-time RT-PCR was carried out using a SYBR Green Realtime PCR Master Mix (Takara Bio, Otsu, Japan) and the Applied Biosystems 7900 real-time PCR detection system (ABI, Foster City, CA, USA). Thermal cycling conditions were as follows: first step, 94°C for 4 min; and the ensuing 40 cycles, 94°C for 1 s, 65°C for 15 s, and 72°C for 30 s. The expression level of each mRNA was normalized by that of GAPDH mRNA. Primers used for real-time RT-PCR are shown in Table 1.

Inoculation of NCI-H2052 cells. Nude BALB/c-*nu/nu* mice (male, 6 weeks old) were obtained from Japan SLC (Shizuoka, Japan). NCI-H2052 cells (1×10^7 cells) suspended in 200 μL culture medium with 50% (v/v) Matrigel (BD Biosciences, San Jose, CA, USA) was inoculated s.c. into the right flank of mice under pentobarbital general anesthesia. Paclitaxel and HUHS1015 were diluted with a physiological salt solution, and i.p. injection of a physiological salt solution, paclitaxel, or
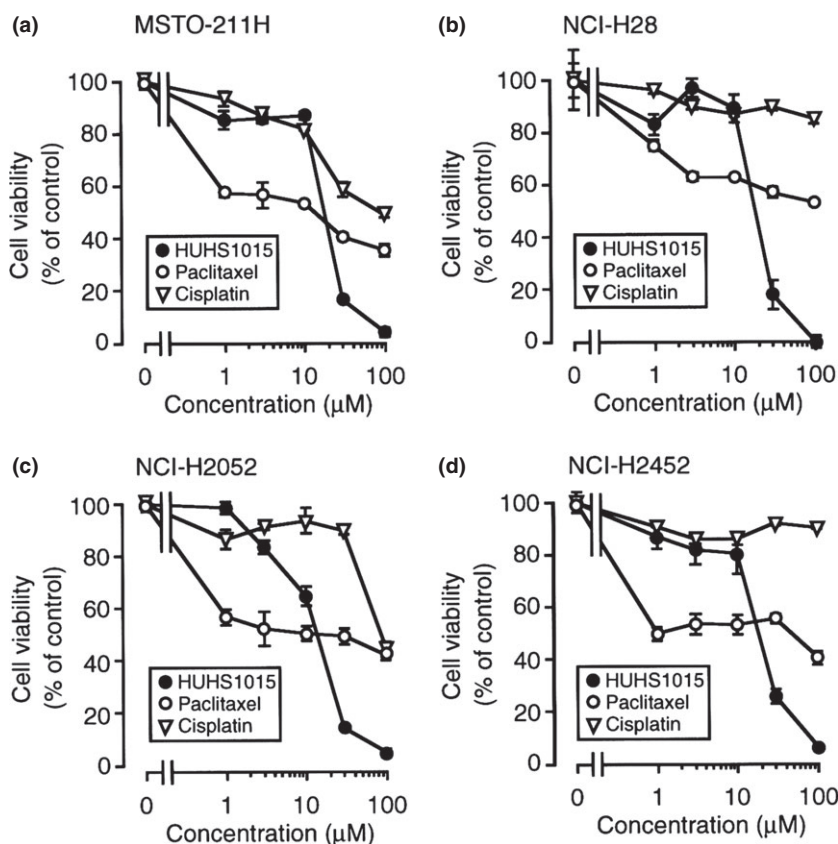

Fig. 2. Effect of HUHS1015 on malignant pleural mesothelioma cell viability. MSTO-211H (a), NCI-H28 (b), NCI-H2052 (c), and NCI-H2452 cells (d) were treated with HUHS1015, paclitaxel, or cisplatin at concentrations as indicated for 24 h, and cell viability was quantified with an MTT assay. Data represent the mean (±SEM) percentage of basal levels (MTT intensities of untreated cells) (*n* = 4 independent experiments).

HUHS1015 twice a week was started 1 week after inoculation. The longer (L) and shorter length (S) of inoculated tumors was measured using calipers and tumor volume (V) was calculated according to the following equation: $V = L \times S^2 \times 1/2$.

Statistical analysis. Statistical analysis was carried out using an unpaired *t*-test and Fisher's protected least significant difference test.

Results

HUHS1015 reduces cell viability of malignant pleural mesothelioma cell lines. HUHS1015 reduced the cell viability of all the investigated malignant pleural mesothelioma cell lines, MSTO-211H, NCI-H28, NCI-H2052, and NCI-H2452, in a concentration (1–100 μM)-dependent manner; a drastic effect was found at concentrations more than 30 μM, with the viability reaching almost 0% of basal levels at 100 μM (Fig. 2). The anticancer drug paclitaxel apparently reduced cell viability of all the investigated malignant pleural mesothelioma cell lines at concentrations higher than 1 μM, reaching 40–50% of basal levels at 100 μM (Fig. 2). Another anticancer drug, cisplatin, reduced the viability of malignant pleural mesothelioma cells by a much lesser extent than paclitaxel (Fig. 2). Collectively, these results suggest that HUHS1015 induces malignant pleural mesothelioma cell death effectively at concentrations higher than 30 μM.

HUHS1015 increases the proportion of the sub-G$_1$ phase of cell cycling in NCI-H2052 and MSTO-211H cells. In the cell cycle analysis by flow cytometry, HUHS1015 increases the proportion of sub-G1 phase NCI-H2052 and MSTO-211H cells (Fig. 3a,c), indicating that HUHS1015 induces apoptosis of these cell lines. HUHS1015 (10 μM) increased the proportion of the G$_1$ and S phases of cell cycling and decreased that of the G$_2$/M phase in NCI-H2052 cells (Fig. 3a). The drug also decreased the proportion of the G$_1$ phase without affecting that of the S and G$_2$/M phases in MSTO-211H cells (Fig. 3c). This suggests no common effect of HUHS1015 on cell cycling among malignant pleural mesothelioma cells.

Paclitaxel (10 μM) significantly increased the proportion of sub-G$_1$ phase in MSTO-211H cells (Fig. 3d), but not in NCI-H2052 cells (Fig. 3b). This indicates that paclitaxel induces apoptosis in MSTO-211H cells. In contrast, paclitaxel (10 μM) markedly increased the proportion of the G$_2$/M phase of cell cycling, but decreased that of the G$_1$ phase in NCI-H2052 cells (Fig. 3b); no such effect was obtained in MSTO-211H cells (Fig. 3d). This indicates that paclitaxel suppresses cell growth by arresting cell cycling at the G$_2$/M phase in NCI-H2052 cells.
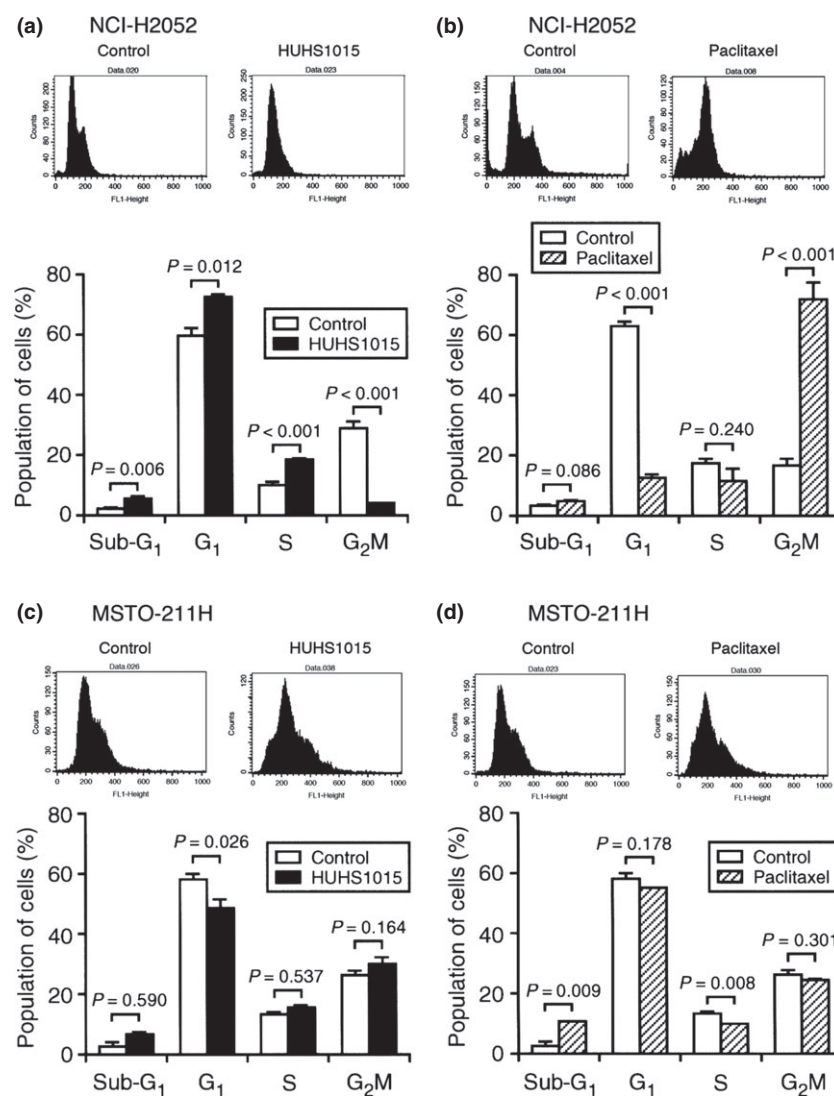

Fig. 3. Cell cycle analysis of NCI-H2052 (a, b) and MSTO-211H cells (c, d) not treated (Control) or treated with HUHS1015 (10 μM) or paclitaxel (10 μM) for 24 h. Typical profiles are shown in upper columns. In the graphs, each column represents the mean (±SEM) percentage for each phase of cell cycling (*n* = 4 independent experiments). *P*-values, unpaired *t*-test.

HUHS1015 induces necrosis and apoptosis of NCI-H2052 and MSTO-211H cells. In the flow cytometry analysis using PI and annexin V, PI is a marker of dead cells and annexin V, detecting externalized phosphatidylserine residues, is a marker of apoptotic cells.[3] In this assay, each population of PI-positive and annexin V-negative, PI-negative and annexin V-positive, or PI-positive and annexin V-positive cells corresponded to primary necrosis, early apoptosis, and late apoptosis/secondary necrosis, respectively.[4] HUHS1015 (15 μM) increased the populations of PI-positive and annexin V-negative, PI-negative and annexin V-positive, and PI-positive and annexin V-positive

cells both in NCI-H2052 (Fig. 4a,b) and MSTO-211H cells (Fig. 4d,e), suggesting that HUHS1015 induces both necrosis and apoptosis of NCI-H2052 and MSTO-211H cells.

Paclitaxel (15 μM) also significantly increased the populations of PI-positive and annexin V-negative, PI-negative and annexin V-positive, and PI-positive and annexin V-positive cells, with the largest population for PI-negative and annexin V-positive cells in NCI-H2052 cells (Fig. 4a,c). A significant increase in the proportions of PI-positive and annexin V-negative and PI-positive and annexin V-positive cells was found in MSTO-211H cells (Fig. 4d,f). These results suggest that
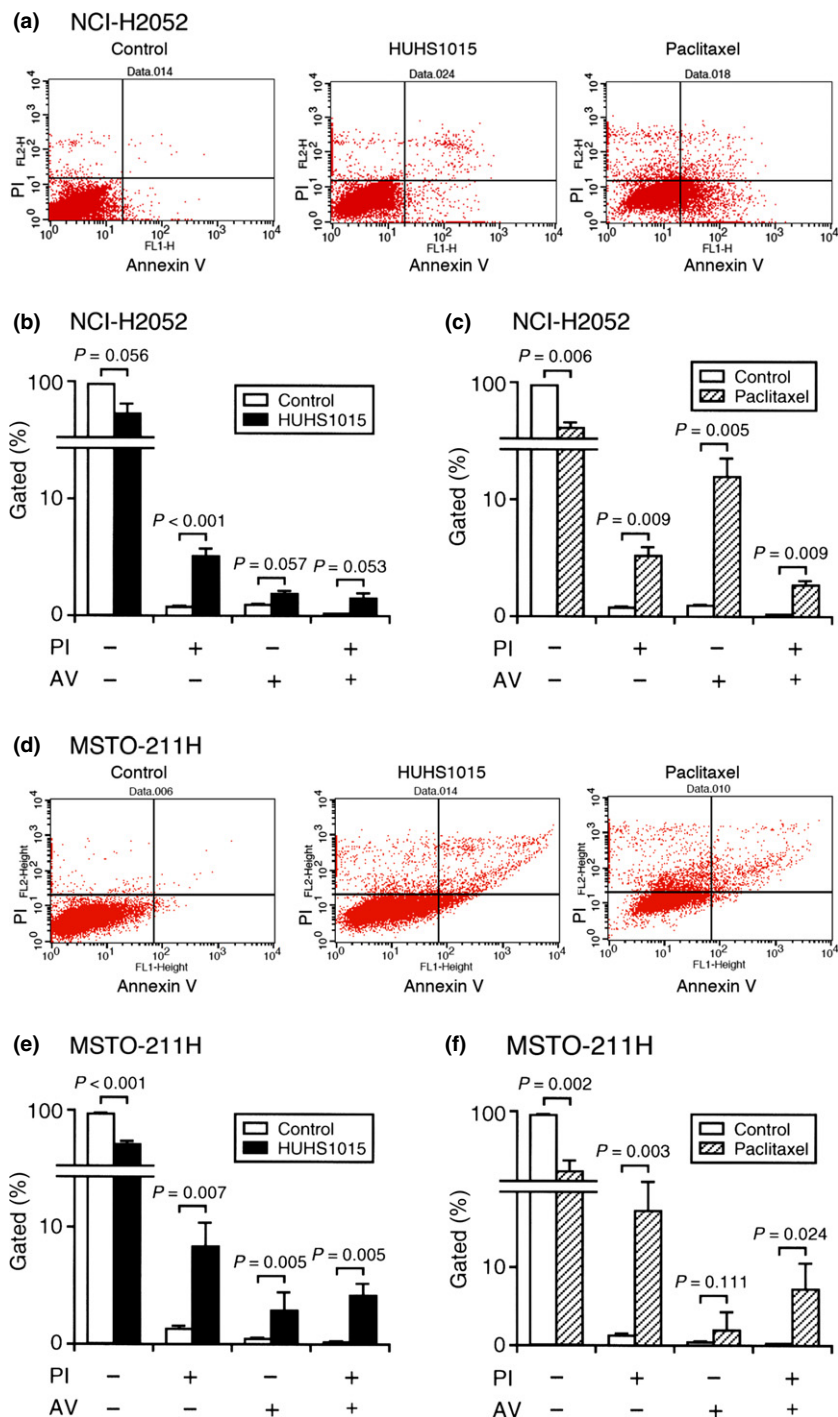

Fig. 4. Flow cytometry using propidium iodide (PI) and annexin V–FITC (AV). NCI-H2052 (a–c) or MSTO-211H cells (d–f) were not treated (Control) or treated with HUHS1015 (15 μM) or paclitaxel (15 μM) for 24 h. Typical profiles are shown in (a) and (d). In the graphs, each column represents the mean (±SEM) percentage of cells in four fractions against total cells (n = 4 independent experiments). P-values, unpaired t-test.

paclitaxel is also implicated both in necrosis and apoptosis of NCI-H2052 and MSTO-211H cells.

HUHS1015 upregulates expression of mRNAs for Puma, Hrk, and Noxa in NCI-H2052 and MSTO-211H cells. To see the effect of HUHS1015 on expression of Bcl-2 family mRNAs, real-time RT-PCR was carried out in NCI-H2052 and MSTO-211H cells. For NCI-H2052 cells, HUHS1015 (15 μM) upregulated

expression of mRNAs for Bax, Puma, and Noxa in a bell-shaped treatment time (2–12 h)-dependent manner, reaching its peak at 6 h (Fig. 5b,d,f), and Hrk in a treatment time-dependent manner (Fig. 5e), whereas expression of mRNAs for Bad, Bid, Bcl-2, Bcl-X_L, and Mcl-1 was not affected (Fig. 5a,c,g–i). For MSTO-211H cells, HUHS1015 (15 μM) upregulated expression of mRNAs for Puma, Hrk, and Noxa in a treatment
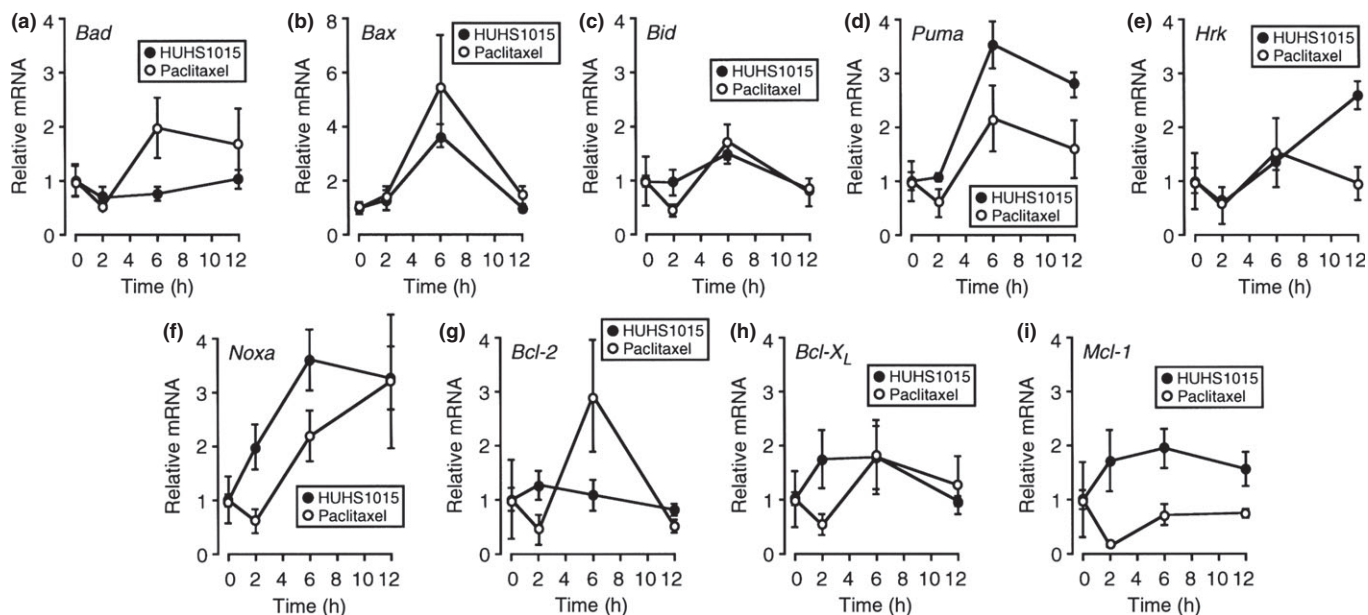

Fig. 5. Real-time RT-PCR analysis of NCI-H2052 cells treated with HUHS1015 (15 μM) or paclitaxel (15 μM) for periods of time as indicated. The mRNA quantity for each gene was calculated from the standard curve made by amplifying different amounts of the GAPDH mRNA, and normalized by regarding the average of independent basal mRNA quantity at 0 h as 1. In the graphs, each point represents the mean (±SEM) ratio relative to basal mRNA levels (*n* = 4 independent experiments).
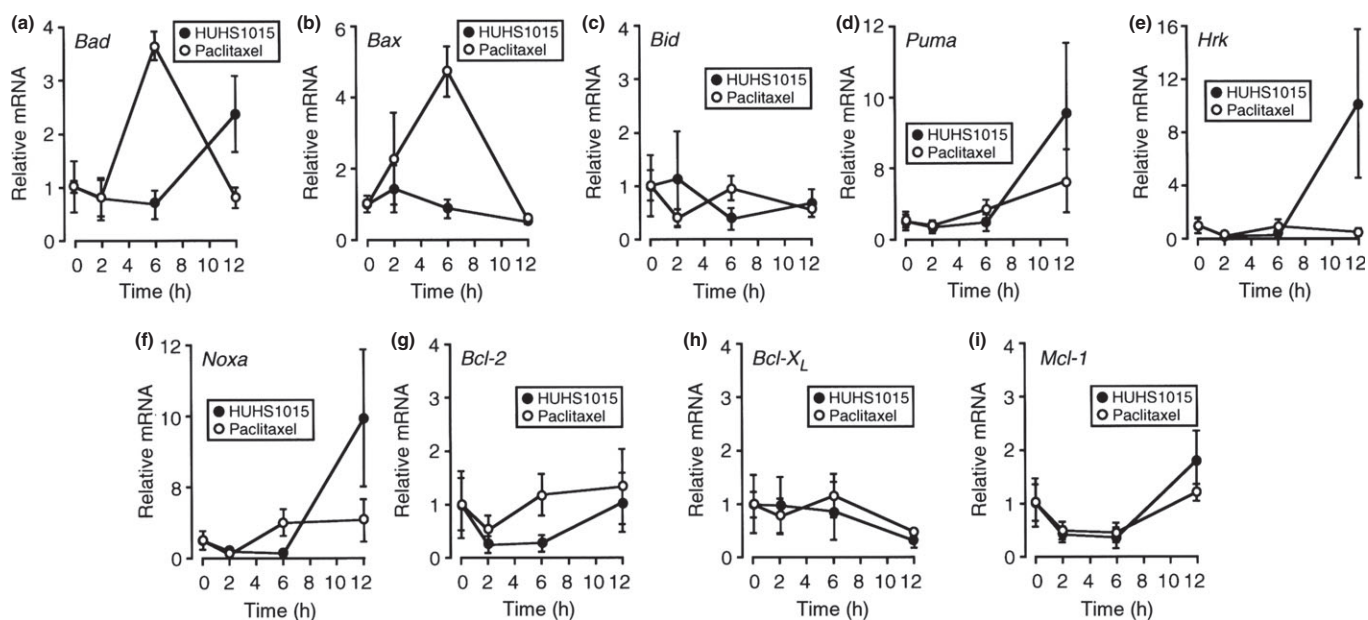

Fig. 6. Real-time RT-PCR analysis of MSTO-211H cells treated with HUHS1015 (15 μM) or paclitaxel (15 μM) for periods of time as indicated. The mRNA quantity for each gene was calculated from the standard curve made by amplifying different amounts of the GAPDH mRNA, and normalized by regarding the average of independent basal mRNA quantity at 0 h as 1. In the graphs, each point represents the mean (±SEM) ratio relative to basal mRNA levels (*n* = 4 independent experiments).

time (2–12 h)-dependent manner (Fig. 6d–f), but no remarkable effect on expression of mRNAs for Bad, Bax, Bid, Bcl-2, Bcl-X_L, or Mcl-1 was obtained (Fig. 6a–c,g–i). Collectively, these results suggest that HUHS1015 induces mitochondria-mediated apoptosis of NCI-H2052 and MSTO-211H cells.

For NCI-H2052 cells, paclitaxel (15 μM) upregulated expression of mRNAs for Bax and Bcl-2 in a bell-shaped treatment time (2–12 h)-dependent manner, reaching its peak at 6 h (Fig. 5b,g), and Noxa in a treatment time-dependent manner (Fig. 5f). However, expression of mRNAs for Bad, Bid, Puma, Hrk, Bcl-X_L, and Mcl-1 was not affected (Fig. 5a,c–e,h, i). For MSTO-211H cells, paclitaxel (15 μM) upregulated expression of mRNAs for Bad and Bax in a bell-shaped treatment time (2–12 h)-dependent manner, reaching its peak at 6 h (Fig. 6a,b), but paclitaxel otherwise had little effect on expression of mRNAs for Bid, Puma, Hrk, Noxa, Bcl-2, Bcl-X_L, and Mcl-1 (Fig. 6c–i). Taken together, these results suggest that the mitochondrial pathway participates, in part, in paclitaxel-induced apoptosis of NCI-H2052 and MSTO-211H cells.

HUHS1015 suppresses proliferation of NCI-H2052 cells. We finally examined the effect of HUHS1015 on NCI-H2052 cell proliferation using mice inoculated with NCI-H2052 cells. Intraperitoneal injection with HUHS1015 at a dose of 9.15 mg /kg, corresponding to approximately 25 μM, twice a week significantly inhibited NCI-H2052 cell growth compared with that for control mice without HUHS1015 ($P < 0.001$, Fisher's protected least significant difference test) (Fig. 7a). All the mice treated with HUHS1015 survived 8 weeks after the beginning of HUHS1015 injection (Fig. 7b) and HUHS1015 had no effect on body weight (Fig. 7c). In addition, we have not confirmed apparent side-effects of HUHS1015 throughout these experiments. These results indicate that HUHS1015 could exert its beneficial anticancer effect on malignant pleural mesothelioma.

Discussion

In the present study, HUHS1015 reduced cell viability in all the investigated malignant pleural mesothelioma cell lines in a concentration (1–100 μM)-dependent manner, reaching almost 0% of basal levels at 100 μM. Paclitaxel, which serves as a mitotic inhibitor, is widely used in chemotherapy for a variety of cancers such as lung, ovarian, breast, thyroid, and pancreatic cancers.[5–10] Cisplatin is a platinum-compound chemotherapy drug that acts as an alkylating agent and is used for treatment of testicular, bladder, ovarian, and lung cancers, as well as several other cancers. Paclitaxel and cisplatin also reduced malignant pleural mesothelioma cell viability in a concentration (1–100 μM)-dependent manner, but the potential for these drugs, especially cisplatin, at concentrations higher than 30 μM was much weaker than that for HUHS1015. This suggests that HUHS1015 at higher concentrations shows beneficial effect on treatment of malignant pleural mesothelioma.

HUHS1015 increased the proportion of the sub-G_1 phase of cell cycling in NCI-H2052 and MSTO-211H cells. This indicates that HUHS1015 induces apoptosis of these cell lines. In addition, HUHS1015 increased the proportion of the G_1 and S phases of cell cycling in NCI-H2052 cells, but such effect was not found in MSTO-211H cells. This suggests that HUHS1015 induces cell cycle arrest at the G_1 and S phases in NCI-H2052 cells, but not in MSTO-211H cells. Paclitaxel increased the proportion of the sub-G_1 phase of cell cycling only in MSTO-211H cells. In contrast, paclitaxel induced marked increases in
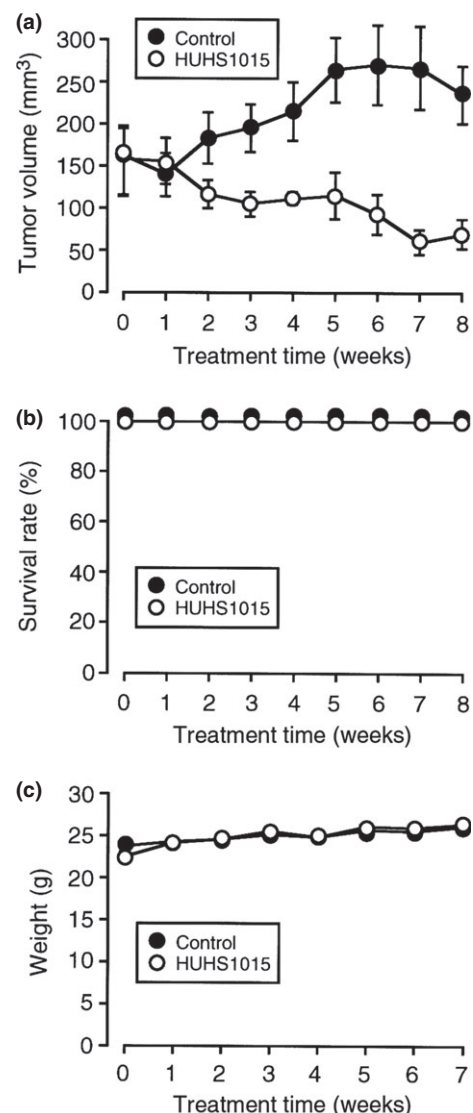

Fig. 7. Suppression of NCI-H2052 tumor growth in mice induced by HUHS1015. NCI-H2052 cells were inoculated s.c. into the flank of mice, and a week later a physiological salt solution (Control) or HUHS1015 (9.15 mg/kg) was injected i.p. twice a week. (a) Tumor volume (mean ± SEM) ($n = 6$ independent mice). (b) Survival rate (the mean ± SEM) ($n = 6$ independent mice). (c) Body weight (mean ± SEM) ($n = 6$ independent mice).

the proportion of the G_2/M phase of cell cycling only in NCI-H2052 cells. This indicates that paclitaxel induces apoptosis of MSTO-211H cells and cell cycle arrest at the G_2/M phase in NCI-H2052 cells.

HUHS1015 increased the population of PI-positive and annexin V-negative, PI-negative and annexin V-positive, and PI-positive and annexin V-positive cells in NCI-H2052 and MSTO-211H cells, which corresponds to primary necrosis, early apoptosis, and late apoptosis/secondary necrosis, respectively.[4] A similar effect was also obtained with paclitaxel. Taken together, these results indicate that HUHS1015 and paclitaxel could induce both necrosis and apoptosis of malignant pleural mesothelioma cells.

In the real-time RT-PCR analysis, HUHS1015 upregulated expression of mRNAs for Bax, Puma, Hrk, and Noxa in NCI-H2052 cells and for Puma, Hrk, and Noxa in MSTO-211H

cells. Paclitaxel upregulated expression of mRNAs for Bax, Noxa, and Bcl-2 in NCI-H2052 cells and for Bad and Bax in MSTO-211H cells. The Bcl-2 family is further divided into three classes: (i) Bcl-2 subfamily that includes Bcl-2, Bcl-X$_L$, Bcl-w, Mcl-1, and A1; (ii) Bax subfamily that includes Bax, Bak, and Bok; and (iii) BH3-only Bcl-2 family that includes Bad, Bik, Bid, Bim, Blk, Hrk, BNIP3, Puma, and Noxa. The Bcl-2 subfamily serves as an anti-apoptotic factor, but the Bax subfamily and BH3-only Bcl-2 family serve as a pro-apoptotic factors.[11,12] Overall, HUHS1015 appears to induce apoptosis of malignant pleural mesothelioma cells through the mitochondria-mediated pathway. Furthermore, paclitaxel might also induce mitochondria-mediated apoptosis of malignant pleural mesothelioma cells, even though paclitaxel upregulated expression of the mRNA for the anti-apoptotic factor Bcl-2 in NCI-H2052 cells.

In the *in vivo* experiments using mice inoculated with NCI-H2052 cells, HUHS1015 strongly suppressed tumor growth, and the survival rate was 100% 8 weeks after the start of HUHS1015 injections. This suggests that HUHS1015 has the potential to effectively suppress proliferation of malignant pleural mesothelioma.

In summary, the results of the present study show that HUHS1015 induces apoptosis of malignant pleural mesothelioma cells, possibly mediated through mitochondria, and in part, cell cycle arrest, thereby leading to suppression of tumor proliferation. This may mean that HUHS1015 could be developed as a promising anticancer drug for treatment of malignant pleural mesothelioma.

Acknowledgment

Disclosure Statement

The authors have no conflict of interest.

References

1 Masachika E, Kanno T, Nakano T, Gotoh A, Nishizaki T. Naftopidil induces apoptosis in malignant mesothelioma cell lines independently of α$_1$-adrenoceptor blocking. *Anticancer Res* 2013; **33**: 887–94.

2 Kanno T, Tanaka A, Shimizu T, Nakano T, Nishizaki T. 1-[2-(2-Methoxyphenylamino)ethylamino]-3-(naphthalene-1-yloxy)propan-2-ol as a potential anticancer drug. *Pharmacology* 2013; **91**: 339–45.

3 Vanags DM, Pörn-Ares MI, Coppola S, Burgess DH, Orrenius S. Protease involvement in fodrin cleavage and phosphatidylserine exposure in apoptosis. *J Biol Chem* 1996; **271**: 31075–85.

4 Pietra G, Mortarini R, Parmiani G, Anichini A. Phases of apoptosis of melanoma cells, but not of normal melanocytes, differently affect maturation of myeloid dendritic cells. *Cancer Res* 2001; **61**: 8218–26.

5 Blanco E, Ferrari M. Emerging nanotherapeutic strategies in breast cancer. *Breast* 2014; **23**: 10–8.

6 Leamon CP, Lovejoy CD, Nguyen B. Patient selection and targeted treatment in the management of platinum-resistant ovarian cancer. *Pharmgenomics Pers Med* 2013; **6**: 113–25.

7 Yardley DA. nab-Paclitaxel mechanisms of action and delivery. *J Control Release* 2013; **170**: 365–72.

8 Cesca M, Bizzaro F, Zucchetti M, Giavazzi R. Tumor delivery of chemotherapy combined with inhibitors of angiogenesis and vascular targeting agents. *Front Oncol* 2013; **3**: 259.

9 Denaro N, Nigro CL, Russi EG, Merlano MC. The role of chemotherapy and latest emerging target therapies in anaplastic thyroid cancer. *Onco Targets Ther* 2013; **9**: 1231–41.

10 Ma WW, Hidalgo M. The winning formulation: the development of paclitaxel in pancreatic cancer. *Clin Cancer Res* 2013; **19**: 5572–9.

11 Zhang LN, Li JY, Xu W. A review of the role of Puma, Noxa and Bim in the tumorigenesis, therapy and drug resistance of chronic lymphocytic leukemia. *Cancer Gene Ther* 2013; **20**: 1–7.

12 Tomek M, Akiyama T, Dass CR. Role of Bcl-2 in tumour cell survival and implications for pharmacotherapy. *J Pharm Pharmacol* 2012; **64**: 1695–702.